An Unsupervised Wi-Fi FTM Ranging Calibration and Positioning Robust to LOS/NLOS Conditions

Takamichi Suruga
Faculty of Science and Technology
Sophia University
Tokyo, Japan
t-suruga-9w5@eagle.sophia.ac.jp

Masakatsu Ogawa
Faculty of Science and Technology
Sophia University
Tokyo, Japan
m-ogawa@sophia.ac.jp

***Abstract*— Wi-Fi Fine Timing Measurement (FTM) measurements contain a constant error that depends on the device and the environment. Previous studies, which we refer to as conventional methods, corrected these errors by calculating the difference between the actual distance and the measured distance obtained from prior measurements; however, this method is labor-intensive and cannot adapt to changes in the device and the environment. In this study, we propose a particle-filter-based positioning method that estimates and corrects the bias in FTM distance in real time and performs positioning using the corrected values. This method eliminates the need for prior measurements while achieving positioning accuracy comparable to or better than conventional methods. To the best of the authors' knowledge, this is the first study to perform real-time calibration using only FTM distance without relying on actual distances. According to the experimental results, under line-of-sight (LOS) conditions between the access point (AP) and the station (STA), the estimated bias converges to the true value over time. Under non-line-of-sight (NLOS) conditions, where a wall exists between the AP and STA, it was confirmed that the estimated bias converges to a value with an additional bias caused by signal penetration through the wall. In terms of positioning accuracy, the proposed method achieved performance comparable to or superior to that of the conventional method.**

Keywords*— *Wi-Fi FTM, Positioning, Particle Filter, Calibration

I. Introduction

In recent years, the development of smartphones and IoT technologies has increased the demand for indoor positioning technologies. In addition to indoor navigation in commercial facilities, real-time tracking and management of equipment, materials, and personnel are required in logistics warehouses and factories. While GPS can provide high-accuracy positioning outdoors, indoor environments often suffer from signal attenuation and reflection caused by building structures, resulting in insufficient accuracy. Therefore, alternative methods are needed. In particular, Wi-Fi-based indoor positioning has gained considerable attention due to its ability to utilize existing Wi-Fi infrastructure. Wi-Fi-based indoor positioning methods can be broadly categorized into two types.

The first type is the fingerprinting method, which utilizes machine learning [1]. In this approach, the received signal strength indicator (RSSI) is measured at many known locations within the target area to construct a database. During positioning, the location is estimated by finding the point in the database that best matches the measured RSSI. This method does not require knowledge of access point (AP) locations and has been reported to achieve relatively high positioning accuracy [2]. However, it requires significant effort and time to construct the database, and its accuracy degrades substantially when the environment changes.

The second type is model-based positioning methods that do not rely on machine learning. Based on ranging between APs and stations (STAs), positions can be estimated using trilateration with three or more APs. Wi-Fi Fine Timing Measurement (FTM), which enables highly accurate distance measurement, is widely used in model-based positioning [3]. In FTM, the round-trip time (RTT) of frames between the AP and the STA is precisely measured, and the distance is calculated by multiplying the RTT by the radio wave propagation speed. In indoor environments representing realistic usage scenarios, particle-filter-based positioning was reported to have an average error of 3.52 m [4]. In addition, positioning methods that integrate other sensor information, such as combining FTM with smartphone-based pedestrian dead reckoning (PDR), have also been studied [5][6].

However, due to hardware processing delays and obstacles, FTM measurements contain a constant bias. Consequently, most prior studies using FTM for indoor positioning, including those mentioned above, perform calibration by measuring the difference between the actual distance and the FTM distance [4]-[9]. While effective at the research stage, this approach poses a significant challenge when implementing services because actual distance measurements are required. Furthermore, since this bias depends on the combination of AP and STA as well as the environment, methods that rely on prior calibration require re-calibration whenever the devices or the environment change.

To address these issues, this paper proposes a particle-filter-based positioning method that estimates and corrects the bias in FTM distance in real time and performs positioning using the corrected values. This approach eliminates the need to measure actual distances and automatically adapts to environmental changes, overcoming the need for re-calibration of previous methods. To the best of the authors' knowledge, this is the first study to perform real-time calibration using only FTM distance without actual distance measurements. The remainder of this paper is organized as follows. Section 2 describes the principles of Wi-Fi FTM, the causes of the ranging errors and conventional calibration methods. Section 3 explains the particle filter used to achieve simultaneous positioning and calibration. Section 4 details the experimental setup, and Section 5 presents the results. Finally, Section 6 concludes the paper.

II. Wi-Fi FTM

A. FTM Algorithm

FTM measures the distance between an AP and a STA, and by deriving the signal propagation time (time-of-flight) from timestamped exchanges, which is then multiplying the signal propagation time by the propagation speed of electromagnetic waves. The FTM procedure begins when the AP receives an FTM Request frame transmitted by the STA

and responds with an ACK frame. Subsequently, the AP sends an FTM frame to the STA and records the transmission time t_1. Upon receiving the FTM frame, the STA records the reception time t_2, sends an ACK frame back to the AP, and records the ACK transmission time t_3. When the AP receives the ACK frame, it records the reception time t_4. The round-trip time (*RTT*) of the frames between the AP and STA is then calculated using these recorded timestamps.

$$RTT = (t_4 - t_1) - (t_3 - t_2) \quad (1)$$

In FTM, this frame exchange is performed N_{FTM} times during a single ranging session to obtain N_{FTM} samples. From these, the measured distance d_{FTM} and standard deviation σ_{FTM} are acquired as follows.

$$d_{FTM} = \frac{c}{2}\frac{1}{N_{FTM}}\left[\sum_{i=1}^{N_{FTM}}\left\{\left(t_{4,i} - t_{1,i}\right) - \left(t_{3,i} - t_{2,i}\right)\right\}\right], \quad (2)$$

$$\sigma_{FTM} = \sqrt{\frac{\sum_{i=1}^{N_{FTM}}\left[\left\{\left(t_{4,i} - t_{1,i}\right) - \left(t_{3,i} - t_{2,i}\right)\right\} - d_{FTM}\right]^2}{N_{FTM}}}. \quad (3)$$

where *c* is the propagation speed of electromagnetic waves in free space.

B. Types of Errors

In general, the distances measured by FTM contain errors. The relationship between the measured distance d_{FTM} and the true distance d_{true} between the AP and STA can be modeled as follows.

$$d_{FTM} = d_{true} + \varepsilon_{delay} + \varepsilon_{NLOS} + \varepsilon_{maltipath} + \varepsilon_{noise} \quad (4)$$

ε_{delay} is the error caused by hardware processing delay [7][8]. When the AP or STA transmits or receives an FTM frame, a small processing delay occurs before the timestamp is recorded. This processing delay increases *RTT*, resulting in a ranging error. This is a constant error that depends on the AP–STA pair. ε_{NLOS} is the error that occurs when obstacles such as walls or doors exist between the AP and STA [8]-[10]. Radio waves propagate more slowly through obstacles than in free air, which increases *RTT* and causes a ranging error. This is a constant error that depends on the positional relationship between the AP and the STA. $\varepsilon_{maltipath}$ is the error caused by multipath propagation. As radio waves reflect, diffract, and transmit through obstacles, the receiver receives frames from multiple paths. Since this error occurs even when measuring with the same AP and STA at the same positions, it is considered a random error. ε_{noise} is the random noise arising from the measurement process.

Based on the above discussion, the errors contained in FTM distance can be broadly classified into two categories. The first is a constant error that does not fluctuate, namely a bias, which depends on the combination and relative positions of the devices, such as the error ε_{delay} caused by hardware processing delay and the error ε_{NLOS} caused by walls and doors between the AP and STA. The second is a random error , which fluctuates randomly, such as the error $\varepsilon_{maltipath}$ due to multipath propagation and the error ε_{noise} due to measurement noise. Here, a bias ε_{bias} and a random error ε_{random} are defined as follows:

$$\varepsilon_{bias} \equiv \varepsilon_{delay} + \varepsilon_{NLOS,} \quad (5)$$

$$\varepsilon_{random} \equiv \varepsilon_{maltipath} + \varepsilon_{noise} \quad (6)$$

Then, (4) can be rewritten as:

$$d_{FTM} = d_{true} + \varepsilon_{bias} + \varepsilon_{random}. \quad (7)$$

This indicates that the error in FTM distance can be decomposed into bias and random error.

C. Conventinal Calibration Method

In conventional research, calibration for the bias included in FTM measurement distances is performed by constructing a polynomial regression model between the measured distance and the true distance. Recently, there are studies that attempt more accurate fitting by setting the maximum order of the explanatory variables to a higher order [5][7], but for this work, we treat the most common model, the linear regression model, as the conventional method. In the linear regression model, the maximum order is set to one. For each AP, the parameters (α, β) are estimated by fitting the calibration data — consisting of the measured and true distances — to the following model:

$$d_{FTM} = \alpha \times d_{true} + \beta. \quad (8)$$

During positioning, calibration is performed for each AP using the obtained parameters (α, β) as follows:

$$\hat{d}_{FTM} = \frac{d_{FTM} - \beta}{\alpha}. \quad (9)$$

III. Particle Filtering

In this study, we employ a particle filter. A particle filter is a method for probabilistically estimating time-varying states [11]. The probability distribution of the state is approximated by a set of *N* particles $\left\{\boldsymbol{X}_t{}^{(i)}, \omega_t{}^{(i)}\right\}_{i=1}^{N}$, each with a state $\boldsymbol{X}_t$ and weight ω_t. In this study, the state $\boldsymbol{X}_t$ is defined as follows to estimate the 2D coordinates of the STA and the bias contained in the FTM distance for each AP.

$$\boldsymbol{X}_t \equiv \left[x, y, \cdots, \varepsilon_{bias,j}, \cdots\right]^T. \quad (10)$$

Here, x and y represent the 2D coordinates of the STA, and $\varepsilon_{bias,j}$ represents the bias in FTM distance for $\mathrm{AP}_j, (j = 1, \ldots, k)$. While previous studies have used particle filters to estimate the STA coordinates [4], to the best of the authors' knowledge, this is the first study to also estimate the bias in FTM distance.

The particle filter consists of the following five steps:

A. Initial Particle Generation

On a 2D plane that includes the target positioning area, *N* particles are generated with a uniform distribution. In this study, *N* was set to 40,000. If *N* is too small, the probability distribution of the state cannot be approximated accurately, resulting in degraded accuracy. Conversely, if *N* is too large, the computational cost increases; therefore, it is essential to choose an appropriate value for N. Additionally, the bias in the FTM distance is initially set to 0 m. That is, each particle has the following state:

$$\boldsymbol{X}_{t=0} = \left[U(x_{min}, x_{max}), U(y_{min}, y_{max}), \cdots, 0, \cdots\right]^T \quad (11)$$

Here, x_{min}, x_{max}, y_{min}, and y_{max} can be set arbitrarily as long as they cover the target positioning area; in this study, they were set to −50 m, 50 m, −50 m, 50 m, respectively. Thereafter, at each time step t, when the measured distance

$d_{FTM,j,t}$ and standard deviation $\sigma_{FTM,j,t}$ are obtained from AP$_j$, the following four steps are executed.

B. Prediction

The state of each particle at time step t is predicted based on the resampled particle states from time step $t-1$ (Details of resampling are provided below). The STA coordinates are predicted based on a standard random walk model [4]. Since abrupt changes in the STA's position are unlikely, it is assumed that the STA moves at a velocity close to its past speed, with a random direction, to estimate the next position. Similarly, abrupt changes in the bias are also unlikely, so it is predicted by adding small noise. Based on the above, the x-coordinate $x_t^{(i)}$, y-coordinate $y_t^{(i)}$ of the STA, and the bias $\varepsilon_{bias,j,t}{}^{(i)}$ in the FTM distance for AP$_j$ of particle i at time step t are predicted as follows.

$$\boldsymbol{X}_t{}^{(i)} = \begin{bmatrix} x_t^{(i)} \\ y_t^{(i)} \\ \vdots \\ \varepsilon_{bias,j,t}{}^{(i)} \\ \vdots \end{bmatrix} = \begin{bmatrix} x_{t-1}^{(i)\prime} + v \cdot \Delta t \cdot \cos\theta \\ y_{t-1}^{(i)\prime} + v \cdot \Delta t \cdot \sin\theta \\ \vdots \\ \varepsilon_{bias,j,t-1}{}^{(i)\prime} + \epsilon \\ \vdots \end{bmatrix}. \quad (12)$$

Here, Δt represents the absolute time difference between time step t and $t-1$. Additionally, the prime symbol ($'$) indicates the state after resampling. Furthermore, v, θ, and ϵ are random numbers that follow the distributions defined below:

$$v \sim \mathcal{N}\left(\mu_{v,t}, \sigma_{v,t}{}^2\right), \quad (13)$$

$$\theta \sim \mathcal{U}(0, 2\pi), \quad (14)$$

$$\epsilon \sim \mathcal{N}\left(0, \sigma_{bias}{}^2\right), \quad (15)$$

where, $\mu_{v,t}$ and $\sigma_{v,t}$ are the mean and standard deviation of the moving speed from the positioning results from time step 1 to $t-1$. $\mathcal{N}(\mu, \sigma^2)$ represents a normal distribution with mean μ and standard deviation μ and $\mathcal{U}(a, b)$ represents a uniform distribution on the interval $[a, b]$. In this study, based on experimental considerations, σ_{bias} was set to 0.03 m.

C. Weighting and Normalization

The weight of each particle $\omega_t^{(i)}$ is updated. Using the measured distance $d_{FTM,j,t}$ and standard deviation $\sigma_{FTM,j,t}$, the likelihood of each particle $L_t^{(i)}$ is calculated as follows:

$$L_t^{(i)} = \prod_{j=1}^{k} \frac{1}{\sqrt{2\pi\sigma_{FTM,j,t}{}^2}} exp\left(-\frac{\left(d_{FTM,j,t} - \hat{d}_{j,t}^{(i)}\right)^2}{2\sigma_{FTM,j,t}{}^2}\right) \quad (16)$$

Here, $\hat{d}_{j,t}^{(i)}$ denotes the expected FTM distance calculated from the coordinates and bias predicted by Section III-B, and it is calculated as follows.

$$\hat{d}_{j,t}^{(i)} = \left\| \begin{bmatrix} x_t^{(i)} \\ y_t^{(i)} \end{bmatrix} - \boldsymbol{\rho}_j \right\| + \varepsilon_{bias,j,t}{}^{(i)} \quad (17)$$

where $\boldsymbol{\rho}_j$ represents the position of the AP$_j$.

Furthermore, the weight $\omega_t^{(i)}$ is obtained by normalizing these likelihoods so that the sum of the likelihoods of all particles equals 1.

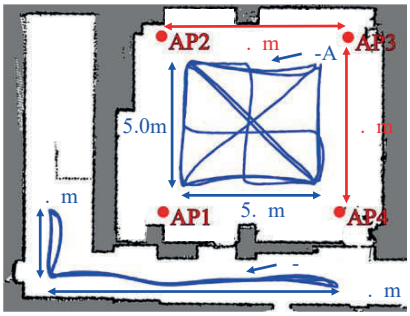

(a) Environment I (APs in room)

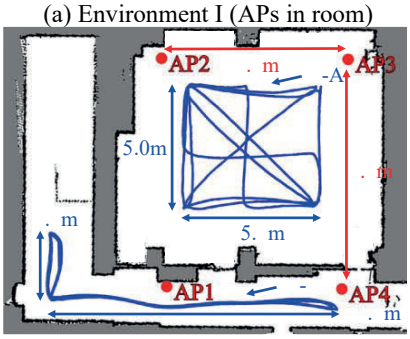

(b) Environment II (APs in room and corridor)

Fig. 1 Measurement environments.

$$\omega_t^{(i)} = \frac{L_t^{(i)}}{\sum_{i=1}^{N} L_t^{(i)}} \quad (18)$$

D. State Estimation

As mentioned previously, the particle filter approximates the state's probability distribution using a set of particles; a statistical aggregation method is necessary to obtain a single state estimate from the particle set. Therefore, in this research, the state at time step t is estimated using the weighted mean of all particles $\overline{\boldsymbol{X}_t}$.

$$\overline{\boldsymbol{X}_t} = \sum_{i=1}^{N} \omega_t^{(i)} \boldsymbol{X}_t^{(i)} \quad (19)$$

This allows the estimation of the STA's 2D coordinates and the bias in the FTM distance for each AP at time step t.

E. Resampling

Repeatedly weighting particles leads to "degeneracy", a problem where the weights become concentrated on a few specific particles, and most other particles no longer contribute to the probability distribution. To solve this issue, resampling is performed. This process prevents the concentration of weights on specific particles by duplicating particles with high weights and eliminating unnecessary particles with low weights. Several resampling methods exist; in this study, resampling is performed using the method known as Multinomial Resampling [12].

In Multinomial Resampling, a cumulative distribution function (CDF) of the weights up to the m-th particle is defined:

$$F_m \equiv \sum_{i=1}^{m} \omega_t^{(i)}. \quad (20)$$

Next, N uniform random numbers are generated in the interval [0, 1]:

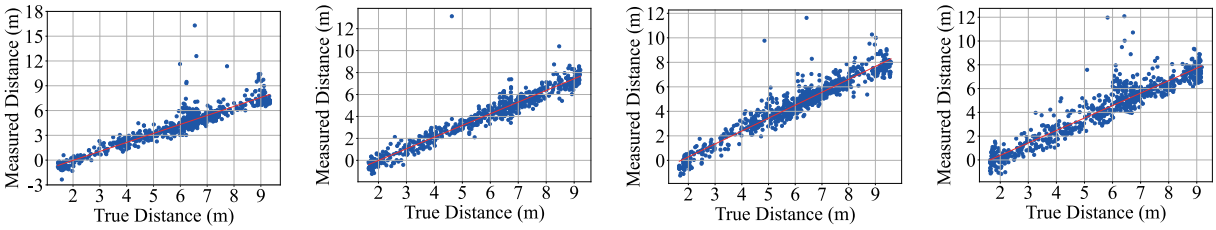

(a) AP1 (LOS) (b) AP2 (LOS) (c) AP3 (LOS) (d) AP4 (LOS)

Fig. 2 FTM ranging results in scenario I-A.

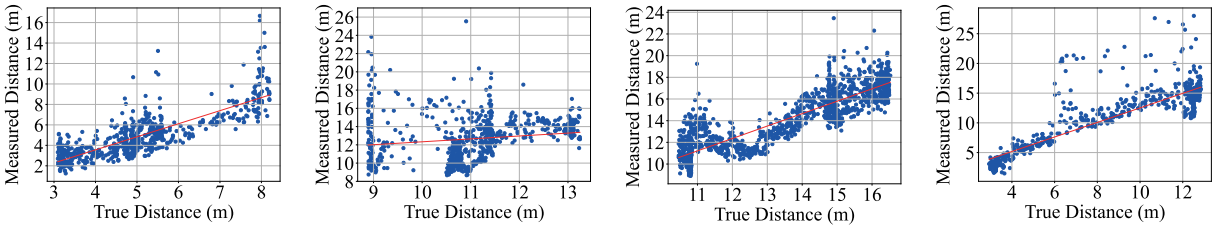

(a) AP1 (NLOS) (b) AP2 (NLOS) (c) AP3 (NLOS) (d) AP4 (NLOS)

Fig. 3 FTM ranging results in scenario I-B.

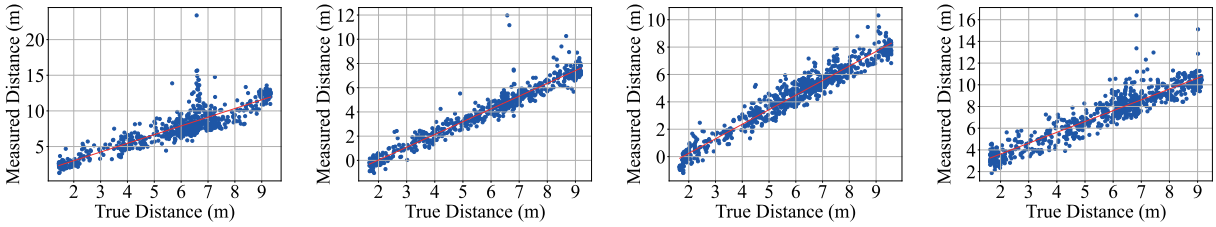

(a) AP1 (NLOS) (b) AP2 (LOS) (c) AP3 (LOS) (d) AP4 (NLOS)

Fig. 4 FTM ranging results in scenario II-A.

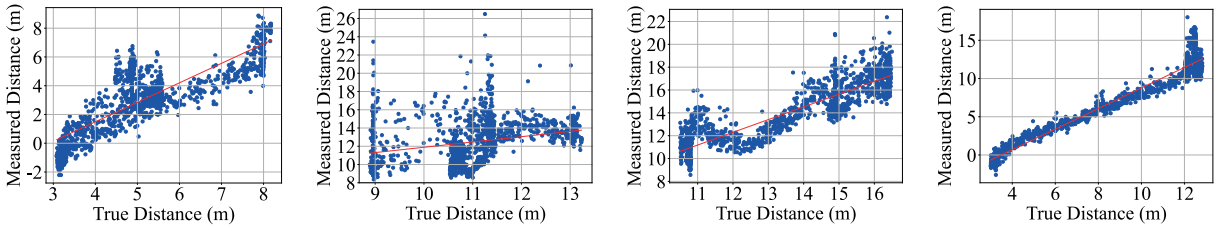

(a) AP1 (LOS) (b) AP2 (NLOS) (c) AP3 (NLOS) (d) AP4 (LOS)

Fig. 5 FTM ranging results in scenario II-B.

$$\mathcal{U}_i \sim \mathcal{U}(0,1),\ i = 1, \ldots, N \tag{21}$$

An index K_i is obtained using the following formula:

$$K_i = min\{m | F_m \geq \mathcal{U}_i\}. \tag{22}$$

Finally, resampling is completed by setting the state of particle with index K_i at time step t, ${\boldsymbol{X}_t}^{(K_i)}$, as the resampled particle state at time step t, ${\boldsymbol{X}_t}^{(i)'}$.

$${\boldsymbol{X}_t}^{(i)'} = \begin{bmatrix} {x_t}^{(i)'} \\ {y_t}^{(i)'} \\ \vdots \\ {\varepsilon_{bias,j,t}}^{(i)'} \\ \vdots \end{bmatrix} = {\boldsymbol{X}_t}^{(K_i)} = \begin{bmatrix} {x_t}^{(K_i)} \\ {y_t}^{(K_i)} \\ \vdots \\ {\varepsilon_{bias,j,t}}^{(K_i)} \\ \vdots \end{bmatrix} \tag{23}$$

IV. Measurement

Fig. 1 (a) shows the setup where the AP is placed only inside the room (Environment I), while Fig. 1 (b) shows the setup where the AP is placed both inside the room and in the corridor (Environment II). There are two types of paths, as indicated by the blue lines in Figs. 1 (a), (b): one is a path that moves randomly within an area of 5.0 m × 5.7 m inside the room (path A), and the other is a path that makes five round trips along an L-shaped corridor measuring 12.2 m × 2.7 m (path B). As there are two types of environments and two types of movement paths, a total of four scenarios (I-A, I-B, II-A, II-B) were conducted for the measurements. Google Wifi was used as the AP, and a Google Pixel 3a was used as the STA. The STA was mounted on an autonomous mobile robot. The robot moved at a maximum speed of 1.0 m/s, and the true positions of the STA were recorded every 100 ms. Both the AP and the STA were placed at a height of 1.2 m from the floor. FTM measurements were performed using the Android application WifiRttScan [13]. N_{FTM} was set to 8. FTM measurements were performed for each AP approximately every 30 ms. According to the principle of

TABLE I. FITTING PARAMATER

Scenario	α				β			
	AP1	AP2	AP3	AP4	AP1	AP2	AP3	AP4
(a) Scenario I-A	1.09	1.06	1.05	1.05	-2.21	-2.13	-1.83	-1.71
(b) Scenario I-B	1.28	0.32	1.15	1.22	-1.55	9.15	-1.38	0.29
(c) Scenario II-A	1.22	1.05	1.06	1.00	0.57	-2.08	-1.89	1.62
(d) Scenario II-B	1.35	0.58	1.11	1.34	-3.93	6.08	-1.07	-4.67

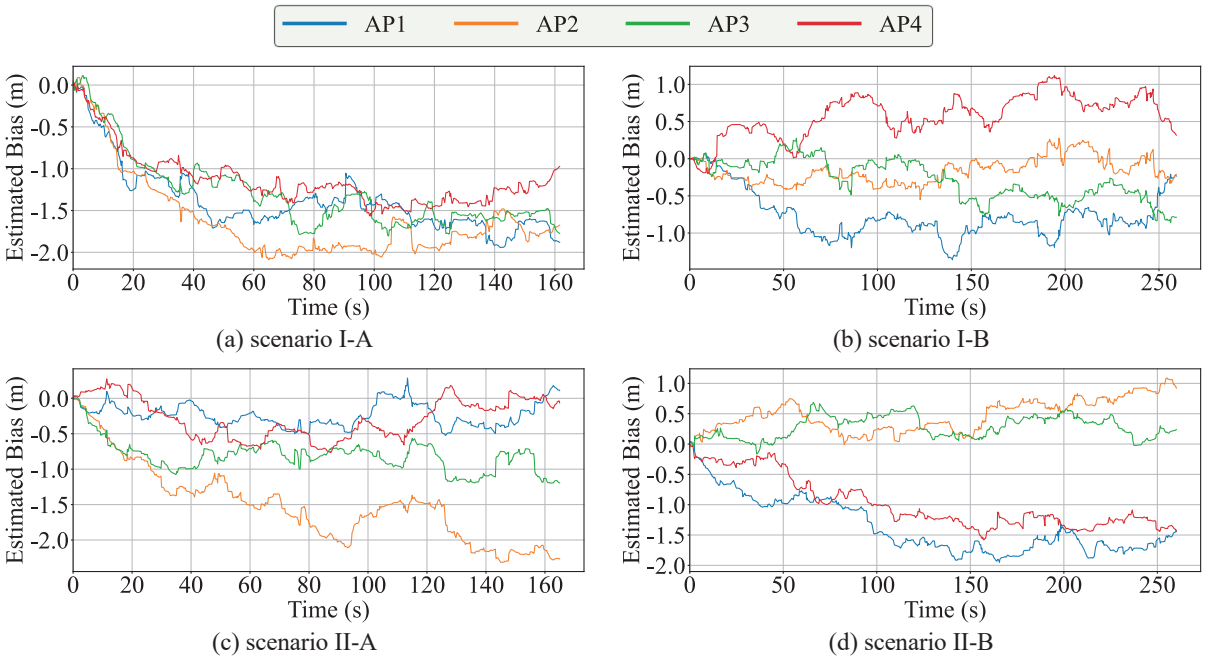

Fig.6 Estimated bias.

trilateration, positioning is impossible unless distances are obtained simultaneously from three or more APs. Therefore, in this study, a 200 ms time window was set, and all measurements obtained within this window were treated as occurring at the same timestamp. The end of the window was used as the measurement timestamp. If multiple distance measurements were obtained from the same AP within the window, their average was used. When measurements from three or more APs were available within the window, the particle filter executed steps (B)–(E) in Section III to estimate the 2D coordinates of the STA and the bias in the FTM distance for each AP.

V. RESULTS

A. FTM Ranging Results

As mentioned earlier, the conventional method requires prior measurements to calibrate the FTM distances. Figs. 2-5 show the FTM ranging results of each AP obtained during the prior measurements in each scenario. The presence of negative measured distances is likely due to the fact that Android devices have a default offset for RTT measurements for each model [14]. The red lines represent the fitted lines obtained by linear regression given in (8), and the obtained parameters (α, β) are shown in Table 1. In scenario I-A, all AP–STA links are line-of-sight (LOS), so multipath effect is minimal, and the measured distance increases linearly with the true distance. In scenario II-A, the measured distances for AP1 and AP4, which is non-line-of-sight (NLOS), can be seen as a parallel shift of those in scenario I-A along the distance axis due to a constant bias ε_{NLOS} is caused by the wall. On the other hand, in scenario I-B and II-B, the measured distance does not increase linearly with the true distance because the effects of wall penetration, diffraction, and multipath vary depending on the STA position.

B. Constant Bias Estimation Results

Fig. 6 shows the estimated bias in the FTM distance for each AP obtained by the particle filter in the positioning experiment in each scenario. In all scenarios, it can be observed that the estimated bias takes some time to converge from the initial value of 0 m. From Figs. 6 (a)-(d), the convergence times are approximately 50 s, 70 s, 40 s, and 100 s, respectively.

For APs that are always in LOS conditions, such as all APs in scenario I-A and AP2 and AP3 in scenario II-A, the estimated bias converges to values close to the β obtained in Section V-A. This indicates that the bias contained in the FTM distances of LOS APs is being accurately estimated. In contrast, AP1 and AP4 in scenario II-A are in NLOS conditions, and their estimated biases converge to higher values compared with the LOS APs. This is reasonable, since the measured distances of NLOS APs are expected to include an additional bias caused by wall attenuation; thus, the larger estimated bias can be interpreted as correctly reflecting this effect. Similarly, in scenario II-B, the estimated biases for AP2 and AP3, which are always in NLOS conditions,

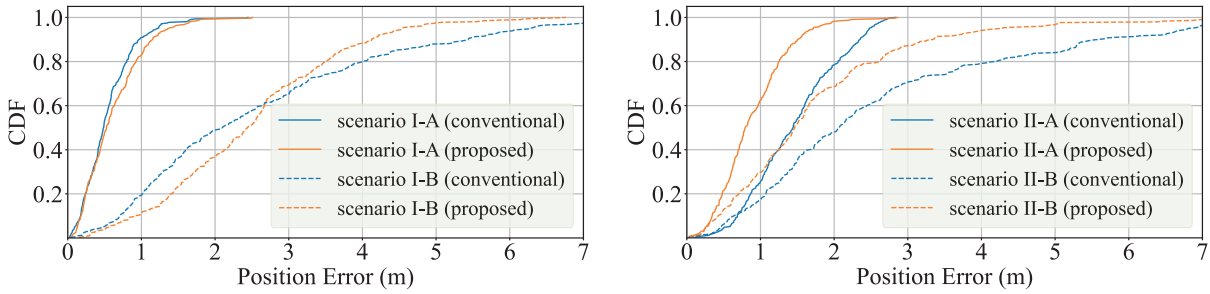

(a) Environment I (b) Environment II

Fig.7 CDF of positioning error after convergence.

converge to higher values than those for AP1 and AP4, which are only partially NLOS. From these results, it can be concluded that when the AP–STA link is always LOS, the bias can be accurately estimated, whereas under NLOS conditions, the estimated bias includes the bias caused by NLOS effects.

C. *Positioning Error*

We compare the positioning accuracy of the proposed method with the conventional method, which corrects FTM distances using (9) and Table 1 and estimates only the STA coordinates with a particle filter. As shown in Section V-B, the proposed method requires some time for bias convergence; therefore, Fig. 7 shows the cumulative distribution function (CDF) of the positioning error after convergence for each environment. Fig. 7 (a) shows results for environment I, and Fig. 7 (b) for environment II. In Fig. 7 (a), for scenario I-A, 80 % of the positioning error was 0.80 m for the conventional method and 0.93 m for the proposed method, showing only a negligible difference. For scenario I-B, the errors were 4.02 m and 3.50 m, respectively, where the proposed method performed better. In Fig. 7 (b), for scenarios II-A and II-B, the proposed method also achieved higher accuracy, with 80 % of the positioning errors of 1.25 m and 2.61 m compared to 2.05 m and 4.21 m for the conventional method. The proposed method achieves higher positioning accuracy because its estimated bias adapts to environmental changes. The conventional method uses a fixed, pre-determined correction value and cannot respond to variations such as changing walls between the AP and STA. In contrast, the proposed method sequentially estimates the bias, enabling environment-dependent corrections.

VI. Conclusion

In this study, we proposed a particle-filter-based positioning method that estimates and corrects the bias in the FTM distance in real-time, and performs positioning using the corrected values. The bias estimation results showed that the estimated bias converges to the correct value over time under LOS conditions. Under NLOS conditions, it reflects the NLOS-induced bias. Regarding the positioning results, when all APs were placed inside the room, 80% of the positioning error was 0.80 m for the conventional method and 0.93 m for the proposed method during random movement within the room, and 4.02 m and 3.50 m, respectively, during movement along the corridor. On the other hand, when the APs were placed both inside the room and in the corridor, 80% of the positioning error was 2.05 m for the conventional method and 1.25 m for the proposed method during random movement within the room, and 4.21 m and 2.61 m, respectively, during movement along the corridor. These results demonstrate that the proposed method achieves positioning accuracy comparable to or higher than that of the conventional method, while eliminating the need for prior measurements based on ground truth, as required in the conventional approach.

References

[1] L. Polak, S. Rozum, M. Slanina, T. Bravenec, T. Fryza, and A. Pikrakis, "Received Signal Strength Fingerprinting-Based Indoor Location Estimation Employing Machine Learning," *Sensors*, vol. 21, no. 13, p. 4605, Jul. 2021.

[2] T. Yang, A. Cabani, and H. Chafouk, "A Survey of Recent ndoor Localization Scenarios and Methodologies," *Sensors*, vol. 21, no. 23, art. no. 8086, Dec. 2021.

[3] J. Dai, M. Wang, . Wu, J. Shen, and X. Wang, "A Survey of Latest Wi-Fi Assisted ndoor Positioning on Different Principles," *Sensors*, vol. 23, no. 18, art. no. 7961, Sept. 2023.

[4] M. Bullmann, T. Fetzer, F. Ebner, M. Ebner, F. Deinzer, and M. Grzegorzek, "Comparison of .4 GHz WiFi FTM- and RSSI-Based ndoor Positioning Methods in Realistic Scenarios," *Sensors*, vol. 20, no. 16, art. 4515, Aug. 2020.

[5] M. Sun, Y. Wang, S. Xu, H. Qi, and X. Hu, " ndoor Positioning Tightly Coupled Wi-Fi FTM Ranging and PDR Based on the Extended Kalman Filter for Smartphones," *IEEE Access*, vol. 8, pp. 49671–49684, Mar. 2020.

[6] G. Guo, R. Chen, X. Niu, K. Yan, S. Xu, and L. Chen, "Factor Graph Framework for Smartphone Indoor Localization: Integrating Data-Driven PDR and Wi-Fi RTT/RSS Ranging," *IEEE Sens. J.*, vol. 23, no. 11, pp. 12346–12354, Apr. 2023.

[7] L. Rana and J. G. Park, "An Enhanced Indoor Positioning Method Based on RTT and RSS Measurements Under LOS/NLOS Environment," *IEEE Sens. J.*, vol. 24, no. 19, pp. 31417–31430, Oct. 2024.

[8] Y. Yu, R. Chen, L. Chen, G. Guo, F. Ye, and Z. Liu, "Wi-Fi Fine Time Measurement: Data Analysis and Processing for ndoor Localisation," *J. Navig.*, vol. 73, no. 5, pp. 1106–1128, May 2020.

[9] M. Ibrahim, H. Liu, M. Jawahar, V. Nguyen, M. Gruteser, R. Howard, B. Yu, and F. Bai, "Verification: Accuracy Evaluation of WiFi Fine Time Measurements on an Open Platform," in *Proc. 24th Annu. Int. Conf. Mobile Comput. Netw. (MobiCom '18)*, New Delhi, India, Oct. 29–Nov. 2, pp. 417–427, Oct. 2018.

[10] Y. Wu, M. He, W. Li, I. Y. Jian, Y. Yu, L. Chen, and R. Chen, "Wi-Fi fine time measurement–Principles, applications, and future trends: A survey," *Inf. Fusion*, vol. 118, Art. no. 102992, Jun. 2025.

[11] F. Gustafsson, "Particle filter theory and practice with positioning applications," *IEEE Aerosp. Electron. Syst. Mag.*, vol. 25, no. 7, pp. 53–82, Jul. 2010.

[12] T. Li, M. Bolic, and P. M. Djuric, "Resampling Methods for Particle Filtering: Classification, implementation, and strategies," *IEEE Signal Process. Mag.*, vol. 32, no. 3, pp. 70–86, Apr. 2015.

[13] Google, "Android-WifiRttScan," [Online]. Available: https://play.google.com/store/apps/details?id=com.google.android.apps.location.rtt.wifirttscan [Accessed: Aug. 29, 2025].

[14] Android Open Source Project, "Wi-Fi RTT," Android Source. [Online]. Available: https://source.android.com/docs/core/connect/wifi-rtt [Accessed: Aug. 26, 2025].